

Rabbit nasal mucosa: nanospheres coated with polypeptides bound to specific anti-polypeptide IgG are better transported than nanospheres coated with polypeptides or IgG alone

Cristina Porta ^a, Silvia Dossena ^a, Vilma Rossi ^b, Mario Pinza ^b, Dario Cremaschi ^{a,*}

^a *Dipartimento di Fisiologia e Biochimica Generali (Sezione di Fisiologia Generale), Università degli Studi di Milano, Via Celoria 26, I-20133 Milan, Italy*

^b *ACRAF, Angelini Ricerche, P. le della Stazione s.n.c., I-00040 S. Palomba Pomezia, Rome, Italy*

Received 22 November 1999; received in revised form 15 February 2000; accepted 2 March 2000

Abstract

In rabbit nasal mucosa, polypeptides and polypeptide-coated nanospheres are actively transported from lumen to blood by M-cells present in specialized transport areas of the epithelium. The largest transport is shown here to occur when some molecules of the polypeptides coating the nanospheres, after adsorption, are bound to the specific anti-polypeptide IgG, e.g. when insulin is bound to the anti-insulin IgG. The transport kinetics of nanospheres coated by insulin bound to its antibody, as a function of bead concentration or of the antibody/insulin coating ratio, have been analyzed. On this basis it was possible to assess the maximal transport capacity of the epithelium and to calculate the percentage of M-cells involved. © 2000 Elsevier Science B.V. All rights reserved.

Keywords: Polypeptide active transport; Antigen sampling; Antibody; Insulin; M-cell; Transcytosis

1. Introduction

The respiratory mucosa of the upper nasal concha and septum of the rabbit has been shown to transport polypeptides or polypeptide-coated nanospheres actively by receptor-mediated endocytosis. The transport regards mini-quantities of material, occurs for a short time, through M-cells, and is strictly correlated to subepithelial lymphoid aggregates; it seems to display the physiological function of sampling antigens,

so that immune responses can be prepared against possibly harmful external agents [1–7].

M-cells of intestinal Peyer's patches, which display the same function, seem to recognize antibodies (IgM, IgA, IgG) better than other polypeptides and to transport them at a greater rate; moreover, nanospheres coated with poorly transported polypeptides are transferred at the same rate as nanospheres coated with antibodies, provided that a few of the adsorbed polypeptides are bound to antibodies specifically raised against them [8–11].

On this basis, the aim of this paper is: (i) to examine whether M-cells of nasal mucosa display similar preferential selectivity for antibodies, and (ii) to study the maximal transport capacity of this epithelium.

* Corresponding author. Fax: +39-02-70644702;
E-mail: dario.cremaschi@unimi.it

2. Materials and methods

Male New Zealand rabbits (weighing approximately 3 kg) were killed by cervical dislocation and the nasal mucosae from the roof of both nostrils were mechanically excised, washed with Krebs-Henseleit saline at room temperature and mounted on frames between two teflon chambers, with the mucosa corresponding to that covering the upper concha exposed in the window (area: 0.3 cm^2). The two chambers were filled with 1 ml Krebs-Henseleit saline and bubbled with pre-humidified 95% O_2 +5% CO_2 to oxygenate the tissue, maintain the pH at 7.4 and stir the solution. The experiments were carried out at a monitored temperature of $27 \pm 1^\circ\text{C}$; at this temperature the short-circuit current, index of ion transports, and the polypeptide transports are half those measured at 37°C , but the isolated mucosa is stable and viable for hours [6,12]; moreover the nostril temperature is lower than 37°C . The viability of the epithelium was checked at the beginning, during and at the end of each experiment by measuring the trans-epithelial potential difference, as previously reported [1,12].

2.1. Flux measurements

The unidirectional mucosa–submucosa and opposite transports of polypeptide-coated latex nanospheres were determined for 2 h, one on the right and the other on the left mucosa from the same animal (with random combinations), using the protocol previously described [3]. The transports were expressed as fluxes (nanospheres transported $\text{cm}^{-2} \text{ h}^{-1}$: $\text{nan cm}^{-2} \text{ h}^{-1}$). Both fluxes were considered unidirectional, since the maximal concentration of nanospheres reached in the flux chamber was 10^{-4} – 10^{-5} compared with that applied in the opposite donor chamber. The bead concentration in the donor chamber, measured on 10 μl samples taken at the beginning (1 min after contact with the tissue) and at the end of the 2 h experiment, was not significantly different (initial concentration: $3.28 \pm 0.01 \cdot 10^{11}$ nanospheres/ml, $n=220$; final concentration: $3.16 \pm 0.08 \cdot 10^{11}$ nanospheres/ml, $n=220$).

The latex nanoparticles were ‘polybead polystyrene microspheres’ (nominal diameter: $0.5 \mu\text{m}$; actual di-

ameter of the lots used: 0.480 – $0.499 \mu\text{m}$) produced by Polysciences (Warrington, PA, USA). A Lambda 5 spectrophotometer (Perkin Elmer, Norwalk, CT, USA) was used for the concentration measurements (wavelength = 600 nm). To prepare the calibration straight line, the reference bead concentrations were predetermined by a Burkert’s chamber after adequate dilution. The nanospheres transported in the 2 h experiment were measured exclusively by a Burkert’s chamber due to their very low concentration. All the determinations in Burkert’s chamber were performed under observation with an Eclipse E600 dark-field microscope (Nikon Europe, Badhoevedorp, The Netherlands) at a $400\times$ magnification, taking advantage of Tyndall’s effect. With a Burkert’s chamber, obtained in a 1.5 mm thick glass slide, the ratio between the measured and nominal value of the nanosphere number was 1.

The polypeptides were adsorbed on nanoparticles by a method previously set up [3,10]. The polypeptide concentration in the medium used for the adsorption process was $6.5 \cdot 10^{-6} \text{ M}$. Still unbound surface sites were completely blocked with bovine serum albumin (BSA) [3,10]. When a double coating of the nanospheres with antibodies was necessary, a first coating by adsorption with $6.5 \cdot 10^{-6} \text{ M}$ BSA or insulin was performed, after which the still unbound sites were blocked with BSA (as above); the nanospheres were then resuspended in Krebs-Henseleit saline containing anti-BSA or anti-insulin IgG at a concentration $6.5 \cdot 10^{-8} \text{ M}$, namely 1:100 compared with that of BSA or insulin; the suspension was incubated at 4°C for 16 h on an orbital shaker, then spun down at 11 000 rpm (7260 g) for 10 min; the precipitate was resuspended in Krebs-Henseleit saline. In both cases (mono-coating or double coating), the final nanosphere concentration was adjusted to $3.3 \cdot 10^{11}$ nan/ml. The variations in insulin, anti-insulin IgG and nanosphere concentrations are reported in Section 3.

2.2. Materials and salines

BSA, murine monoclonal anti-human insulin immunoglobulin G_1 (anti-ins IgG or IgG_{ins}), murine monoclonal anti-BSA immunoglobulin G_{2a} (anti-BSA IgG or IgG_{BSA}) and rabbit polyclonal anti-BSA immunoglobulin G were supplied by Sigma

(ST. Louis, MO, USA); bovine Na-insulin was supplied by Calbiochem (AG Luzern, Switzerland).

The Krebs-Henseleit solution had the following composition (mM): 142.9 Na⁺, 5.9 K⁺, 2.5 Ca²⁺, 1.2 Mg²⁺, 127.7 Cl⁻, 24.9 HCO₃⁻, 1.2 SO₄²⁻, 1.2 H₂PO₄⁻, 5.5 glucose; pH 7.4. The polypeptide concentration was molal.

2.3. Statistics

The results are expressed as means \pm standard errors (S.E.M.). Student's *t*-test for unpaired or, when possible, for paired data was used for the statistical analysis. Interpolating straight lines and sigmoidal curves were calculated by linear and non-linear regressions.

3. Results

3.1. Transports of BSA, insulin and antibodies

Table 1 reports the measured unidirectional fluxes of nanospheres coated with different polypeptides, whereas Fig. 1 summarizes the corresponding calculated net fluxes, indicating the statistical significance

of the increases in J_{net} , obtained with the different bead coatings, and the relative values of J_{net} with respect to BSA J_{net} .

The nanospheres coated by incubation with $6.5 \cdot 10^{-6}$ M BSA were actually completely covered with BSA, since four washings with 5% BSA followed this incubation, in order to block all the unbound surface sites of the nanosphere. In spite of this fact, the BSA J_{net} was significantly different from zero, but very low (Fig. 1), as previously observed [6]. Conversely net transport was significantly ($P < 0.01$) higher $6\text{--}8 \cdot 10^6$ nan cm⁻² h⁻¹ when the nanospheres were coated in the presence of bovine insulin or antibodies (anti-BSA or anti-insulin IgG) at the concentration of $6.5 \cdot 10^{-6}$ M (Fig. 1). It is noteworthy that under these conditions the nanosphere surface specifically coated is approx. 6%, whereas more than 90% is covered by BSA [6]. After adsorption with BSA or insulin on the nanosphere surface, when these polypeptides were in part (1:100) bound to the corresponding antibodies (incubation with $6.5 \cdot 10^{-8}$ M anti-BSA or anti-insulin IgG), the net nanosphere transport increased in both cases. The values reached were significantly larger than those observed for nanospheres coated with BSA or insulin only, or only with the antibodies directly ad-

Table 1

Transepithelial fluxes of nanospheres coated with BSA, insulin, anti-BSA IgG, anti-insulin IgG, BSA bound to anti-BSA IgG or insulin bound to anti-insulin IgG

	Experiment conditions	<i>n</i>	J_{ms}	J_{sm}
A.	Coating with:			
	1. BSA	11	$6.0 \pm 0.6^{**}$	4.1 ± 0.3
	2. Anti-BSA IgG (monoclonal)	6	$10.1 \pm 1.2^{**}$	4.1 ± 0.3
	3. BSA+anti-BSA IgG (monoclonal)	11	$13.6 \pm 1.3^{**}$	4.0 ± 0.2
	4. BSA+anti-BSA IgG (polyclonal)	6	$13.6 \pm 1.4^{**}$	3.5 ± 0.4
B.	Coating with:			
	1. Insulin	17	$10.2 \pm 0.6^{**}$	3.1 ± 0.2
	2. Anti-insulin IgG	7	$12.0 \pm 1.8^{**}$	4.0 ± 0.5
	3. Insulin+anti-insulin IgG (monoclonal)	22	$64.3 \pm 5.0^{**}$	5.2 ± 0.3
C.	MIA+DNP (coating with insulin+anti-insulin IgG)	7	7.7 ± 2.2	7.4 ± 2.3

After 30 min preincubation, $3.3 \cdot 10^{11}$ /ml polypeptide-coated nanospheres (polystyrene, 0.5 μ m diameter) were added to the mucosal or submucosal compartment; the corresponding total unidirectional transports during a 2 h period were determined by a Burkner chamber and expressed as equivalent fluxes (J_{ms} , J_{sm} ; 10^6 nan cm⁻² h⁻¹). Bead coating was carried out by incubating the nanospheres with the $6.5 \cdot 10^{-6}$ M polypeptide at 37°C for 90 min (mono-coating with BSA, insulin or the respective antibodies alone); when a double coating was required, after the first incubation with BSA or insulin a second subsequent incubation was performed with $6.5 \cdot 10^{-8}$ M anti-BSA or anti-insulin IgG at 4°C overnight. Monoiodoacetate (MIA, $3 \cdot 10^{-3}$ M) and dinitrophenol (DNP, 10^{-4} M), when added, were present on both sides of the tissue during the 2 h measuring period. The results are presented as means \pm S.E.M.; *n*, number of experiments. **, $P < 0.01$ compared with the corresponding J_{sm} .

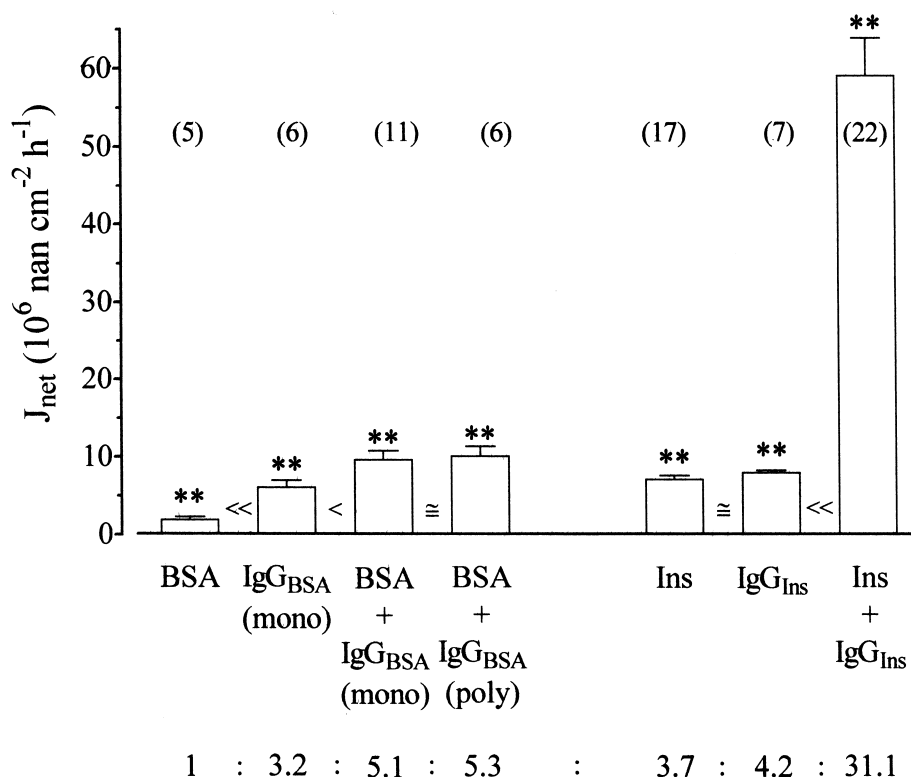


Fig. 1. Net fluxes (J_{net}) of polypeptide-coated nanospheres (histograms) and their ratios to the net flux of BSA-coated nanospheres, taken as a reference. The histograms represent the mean \pm S.E.M. (number of experiments in brackets). **: $P < 0.01$ compared with zero; \cong , $<$, \ll : not significantly different, $P < 0.05$, $P < 0.01$ compared with the preceding histogram.

sorbed on the nanospheres by incubation at a hundred times higher concentration ($6.5 \cdot 10^{-6}$ M) (Fig. 1). Although qualitatively similar effects were obtained with anti-BSA or anti-insulin IgG, quantitatively the increase in transport was much more substantial with anti-insulin IgG (net transport increased to $59 \cdot 10^6 \text{ nan cm}^{-2} \text{ h}^{-1}$ with anti-insulin IgG vs. $10 \cdot 10^6 \text{ nan cm}^{-2} \text{ h}^{-1}$ with anti-BSA IgG). The large net transport so measured with anti-insulin IgG coating was an actual active transport, since moniodoacetate ($3 \cdot 10^{-3}$ M) plus dinitrophenol (10^{-4} M), added on both sides of the epithelium during the 2 h experiment, abolished it (Table 1). When the anti-BSA IgG was changed from monoclonal to polyclonal form, the result did not change (net transport approx. $10 \cdot 10^6 \text{ nan cm}^{-2} \text{ h}^{-1}$ in both cases: Fig. 1).

Fig. 1 also reports the relative values of J_{net} . It increases significantly by 3–4 times when nanospheres are partially coated with insulin or antibodies instead of BSA only; it rises by more than 5 times with BSA bound to mono- or polyclonal anti-BSA

IgG, and by 31 times with insulin bound to anti-insulin IgG. With this latter coating the increase was 8.3 and 7.4 times compared with the J_{net} obtained with insulin or anti-ins IgG coating respectively.

As previously observed [6], the unidirectional sub-mucosa–mucosa flux (passive flux) displayed values which ranged between approx. $3\text{--}5 \cdot 10^6 \text{ nan cm}^{-2} \text{ h}^{-1}$, relatively independently of the nanosphere coating, in agreement with non-specific paracellular permeation through nanolesions of the epithelium, caused for example by simple cell death or edge damage (Table 1). Only after treatment with metabolic inhibitors J_{sm} tended to increase moderately, but the standard error was so large that the increase was not statistically significant. The transepithelial potential difference (V_{sm}) was abolished in parallel (V_{sm} before treatment: $4.6 \pm 0.6 \text{ mV}$; V_{sm} after treatment: $0.0 \pm 0.0 \text{ mV}$).

Finally, it is to emphasize that the transepithelial potential difference was not affected by the transport of the differently coated beads.

3.2. Net transport of nanospheres as a function of nanosphere concentration

After the usual loading with insulin ($6.5 \cdot 10^{-6}$ M) plus anti-insulin IgG ($6.5 \cdot 10^{-8}$ M) at the usual bead concentration ($3.3 \cdot 10^{11}$ nan/ml), nanospheres were diluted or concentrated in Krebs-Henseleit saline and so presented to the mucosa at different concentrations, but with the same loading per nanosphere; thus the kinetics of the two unidirectional (J_{sm} , J_{ms}) fluxes could be measured as a function of bead concentration. Fig. 2 shows that J_{sm} does not display any dependence on bead concentration, at least over $0.02 \cdot 10^{11}$ nan/ml; in fact its data points are interpolated at the best by a straight line ($J = aS + b$; $r^2 = 0.602$, $P < 0.05$), parallel to the abscissa ($a = 0.0 \pm 0.0$ cm h $^{-1}$, $b = 4.5 \pm 0.2 \cdot 10^6$ nan cm $^{-2}$ h $^{-1}$). Conversely, J_{ms} becomes significantly different from J_{sm} over a $0.02 \cdot 10^{11}$ nan/ml concentration and increases significantly as a function of bead concentration, with sigmoidal kinetics ($r^2 = 0.996$; $P < 0.01$); the half-maximal concentration ($S_{0.5}$) is $3.2 \pm 0.1 \cdot 10^{11}$ nan/ml, J_{max} $112.0 \pm 9.5 \cdot 10^6$ nan cm $^{-2}$ h $^{-1}$, Hill number (n_H) 1.7. As a consequence, over the same threshold of concentration the net flux (J_{net} ,

not reported) becomes significantly different from zero and increases sigmoidally with concentration ($r^2 = 0.998$, $P < 0.01$); $S_{0.5}$ is $3.2 \pm 0.1 \cdot 10^{11}$ nan/ml, J_{max} $110.0 \pm 17.7 \cdot 10^6$ nan cm $^{-2}$ h $^{-1}$ and n_H 1.5.

3.3. Different loadings with insulin plus anti-insulin IgG

Nanospheres ($3.3 \cdot 10^{11}$ nan/ml) were coated by incubating with $470 \cdot 10^{-6}$ M insulin (the maximal reachable concentration of soluble bovine insulin). At this concentration approx. 86% of the nanosphere surface is covered by insulin [6]. After four washings with BSA, the nanospheres were incubated with anti-insulin IgG at different concentrations (1:10000 to 1:1000 compared with insulin). Fig. 3a shows that the passive flux J_{sm} is independent of anti-insulin IgG concentration in the concentration range tested. Conversely, J_{ms} and J_{net} (Fig. 3a and b) are not significantly different from those measured with a coating of $470 \cdot 10^{-6}$ M insulin only, when the double coating is performed with $4.7 \cdot 10^{-8}$ M anti-insulin IgG (anti-ins IgG/insulin ratio = 1:10000), but they increase by approx. 8 times ($J_{net} \cong 68.5 \cdot 10^6$ nan cm $^{-2}$ h $^{-1}$) when the double coating is performed

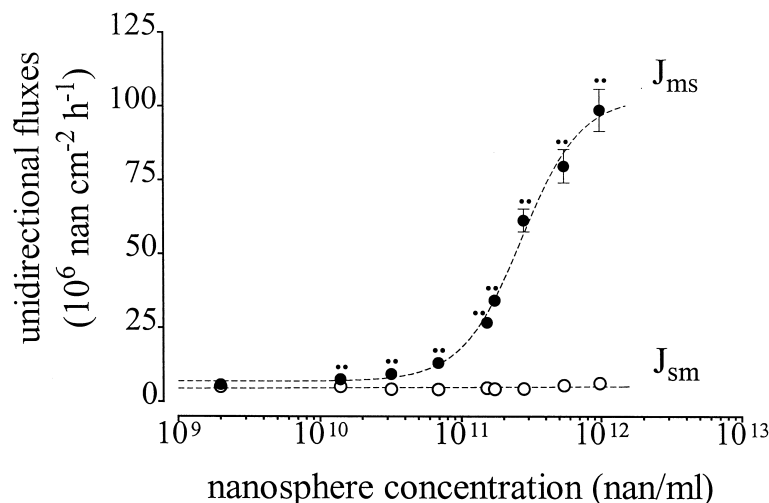


Fig. 2. Unidirectional (J_{ms} , J_{sm}) fluxes of nanospheres, coated with insulin+anti-insulin IgG, as a function of nanosphere concentration. Semilogarithmic scale. Nanospheres ($3.3 \cdot 10^{11}$ nan/ml) were pre-coated with insulin (incubation with $6.5 \cdot 10^{-6}$ M insulin for 90 min at 37°C), then washed with 5% BSA (to cover all the unbound sites on the nanosphere surface) and finally incubated with $6.5 \cdot 10^{-8}$ M anti-insulin IgG, for 16 h at 4°C, to specifically bind antibodies to part of the insulin adsorbed. The nanospheres were then diluted or concentrated as required. The results are presented as means \pm S.E.M. ($n = 6$ for each data point). **: $P < 0.01$ compared with J_{sm} .

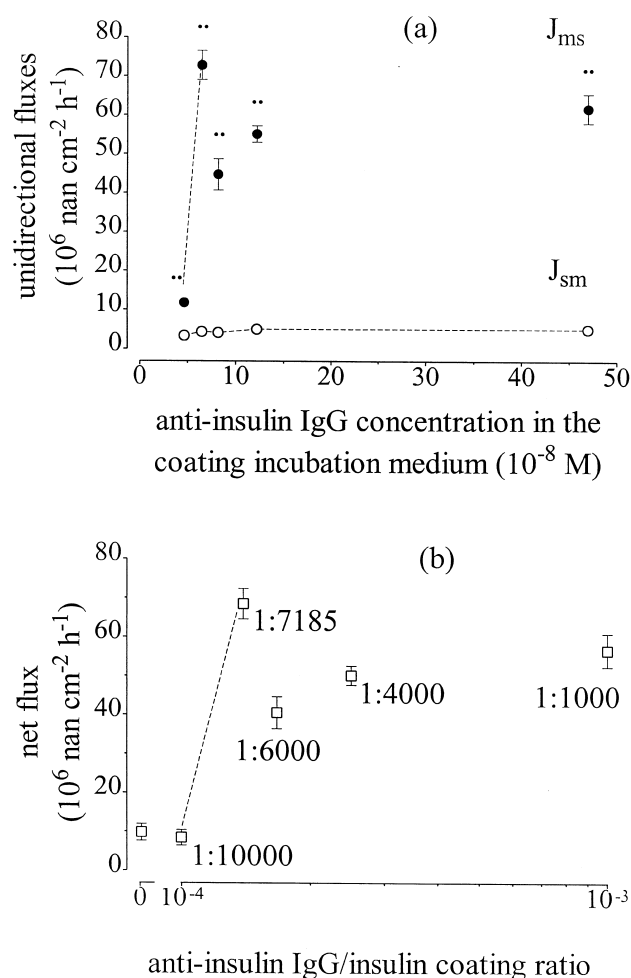


Fig. 3. (a) Unidirectional (J_{ms} , J_{sm}) fluxes of nanospheres coated by subsequent incubations with $470 \cdot 10^{-6} \text{ M}$ insulin and anti-insulin IgG at different concentrations (range: $4.7 \cdot 10^{-8}$ to $47 \cdot 10^{-8} \text{ M}$). (b) Corresponding calculated net fluxes (J_{net}) of nanospheres as a function of the antibody/insulin coating ratio. Nanosphere concentration: $3.3 \cdot 10^{11} \text{ nan/ml}$. The results are presented as means \pm S.E.M. ($n=5$ for each data point); $n=6$ for the net flux of nanospheres coated with $470 \cdot 10^{-6} \text{ M}$ insulin only (ratio=0); **: $P < 0.01$ compared with J_{sm} .

with $6.5 \cdot 10^{-8} \text{ M}$ antibody (anti-ins IgG/insulin ratio=1:7185). This J_{net} value is not significantly different from that obtained by subsequent incubations with $6.5 \cdot 10^{-6} \text{ M}$ insulin and $6.5 \cdot 10^{-8} \text{ M}$ antibody (Fig. 1). With increasing concentrations of antibody over $6.5 \cdot 10^{-8} \text{ M}$ to $47 \cdot 10^{-8} \text{ M}$ (antibody/insulin ratio=1:1000) J_{ms} and J_{net} apparently decrease (Fig. 3a and b), but they are underestimated owing to the formation of many aggregates of the nanospheres transported.

4. Discussion

4.1. Transcytosis stimulation by antibodies

In intestinal Peyer's patches, IgM-, IgA- or IgG-coated nanospheres or virus-antibody complexes have been shown to be much more readily absorbed than nanospheres coated with other polypeptides or than virus alone in M-cells of follicle-associated epithelium; moreover, nanospheres coated with poorly absorbable polypeptides are transported as well as antibody-coated nanospheres if some molecules of the adsorbed polypeptide are bound to a specific anti-polypeptide antibody [8–11]. Thus a non-isotype specific common immunoglobulin domain seems to facilitate bead binding and uptake [11].

In a previous paper we showed that M-cells, present in the nasal respiratory mucosa of the rabbit [7], equally transcytose IgA- or IgG-coated nanospheres more readily than nanospheres coated with other polypeptides, such as BSA or enkephalin; however, they transfer carbocalcitonin- or insulin-coated nanoparticles just as fast [6]. The present paper confirms that insulin-coated beads are transported at the same rate as IgG-coated beads. Thus either the same domain recognized by receptors in antibodies is also present in other kinds of polypeptides, or in nasal mucosa different receptors recognize different amino acid sequences with similar polypeptide receptor affinities.

We have already emphasized that the observed affinities of insulin or antibodies for receptors can only be the apparent affinities of the polypeptides adsorbed on the bead [6]. In fact, the adsorption of the polypeptide on the nanoparticle forces the molecule into positions that do not necessarily represent the best orientation for easy binding to receptors; hence these apparent affinities do not necessarily correspond to the actual affinities of the free polypeptides.

In line with the importance of molecule orientation on the bead surface, we show here that anti-BSA or anti-insulin IgG, bound 1:100 with their F_{ab} to the adsorbed BSA or insulin molecules (and thus with their F_c oriented free in the medium), enhance transports of the nanoparticles so coated to levels not merely equal to (as in intestine), but significantly larger (anti-BSA IgG: $1.6 \times$) or even much larger

(anti-insulin IgG: $7.4\times$) than those achieved with beads directly coated with the corresponding antibodies alone, at 100 times larger concentrations.

These results demonstrate that: (i) the effect of the double coating with bound antibodies is much more substantial in nasal mucosa than in Peyer's patches, (ii) hence orientation and free F_c exposure seem to be more essential to bind antibodies to nasal mucosa receptors, (iii) the non-isotype specific common binding domain in antibodies seems to be located in F_c .

The double coating with monoclonal anti-BSA IgG produced qualitative results similar to those obtained with the double coating with monoclonal anti-insulin IgG; however, the stimulation obtained was much lower, rather than equal, as might have been expected of a common binding domain. The available murine monoclonal anti-BSA and anti-insulin IgG were IgG_{2a} and IgG₁ respectively (see Section 2.2), so the two F_c were different; however, with rabbit polyclonal anti-BSA IgG the result was the same as that obtained with murine monoclonal anti-BSA IgG_{2a}. On this basis, the F_c is likely to be better oriented towards the medium in the bound anti-insulin than anti-BSA IgG, probably dependently on the location of the insulin–antibody binding site on the insulin molecule.

4.2. Maximal transport capacity in the mucosa of the upper concha

The fact remains that the maximal transport observed was obtained by coating beads with insulin plus its antibody. By using this coating we tried to assess the maximal transport capacity of the nasal epithelium in the upper concha: (i) with the standard double bead coating (incubation with $6.5\cdot 10^{-6}$ M insulin and then with $6.5\cdot 10^{-8}$ M anti-insulin IgG) fluxes were measured as a function of bead concentration, (ii) with the standard bead concentration ($3.3\cdot 10^{11}$ nan/ml) fluxes were measured as a function of constant insulin at its maximal degree of coating (incubation with $470\cdot 10^{-6}$ M insulin) plus variable antibody coating (incubation with 4.7 to $47\cdot 10^{-8}$ M anti-insulin IgG).

In the first case the net flux kinetics proved sigmoidal, the half-maximal concentration ($S_{0.5}$) was approx. equal to the standard bead concentration usually used ($3.3\cdot 10^{11}$ nan/ml), and the calculated J_{\max}

was $110\cdot 10^6$ nan cm^{-2} h^{-1} , obtained at the calculated concentration of about 10^{13} nan/ml. Actually the maximal bead concentration which could be used, avoiding large changes in saline viscosity, was $9.8\cdot 10^{11}$ nan/ml, namely only about 3 times the standard concentration; the corresponding net flux was approx. $90\cdot 10^6$ nan cm^{-2} h^{-1} .

In the second case, the maximal measured net transport ($\cong 70\cdot 10^6$ nan cm^{-2} h^{-1}) was obtained at the standard antibody coating concentration ($6.5\cdot 10^{-8}$ M), in spite of the increase in insulin coating concentration from $6.5\cdot 10^{-6}$ to $470\cdot 10^{-6}$ M (which enhances the insulin covering of the nanosphere from 6 to 86% [6]) and the consequent reduction in the antibody/insulin ratio from 1:100 to 1:7185. On the other hand, 6% bead coating with insulin produces 70–80% of the maximal transport which can be obtained with insulin [6], so that an increase in insulin coating is almost useless for the purpose of stimulating transport. Equally, an increase in bound antibody coating, using coating concentrations larger than $6.5\cdot 10^{-8}$ M, only seems to produce a transfer saturation with bead aggregation, probably owing to the bead crowding in the narrow intercellular spaces with cross-linking phenomena between the nanoparticles. Transport abruptly drops with coatings obtained with antibody concentrations just a little smaller than $6.5\cdot 10^{-8}$ M: at $4.7\cdot 10^{-8}$ M IgG, the transport stimulation induced by the presence of the antibody is abolished. Thus an antibody concentration just a little larger than $6.5\cdot 10^{-8}$ M and less than $7.8\cdot 10^{-8}$ M (at which saturation and aggregation are already observed) can probably produce the maximal measurable transport, which should therefore be higher than the measured $70\cdot 10^6$ nan cm^{-2} h^{-1} .

In conclusion, the theoretical maximal capacity of transcytosis is approximately represented by the calculated transport of $110\cdot 10^6$ nan cm^{-2} h^{-1} , but some external factors (viscosity of the donor saline and crowding of nanospheres in intercellular spaces) reduce the actual capacity to about $70\text{--}90\cdot 10^6$ and more probably to $90\cdot 10^6$ nan cm^{-2} h^{-1} . All this is summarized in Fig. 4.

This maximal transport is unlikely to be much modified by the in vivo temperature (about 30–31°C in the nose air and probably 34°C in the epithelium, compared with the experiment temperature

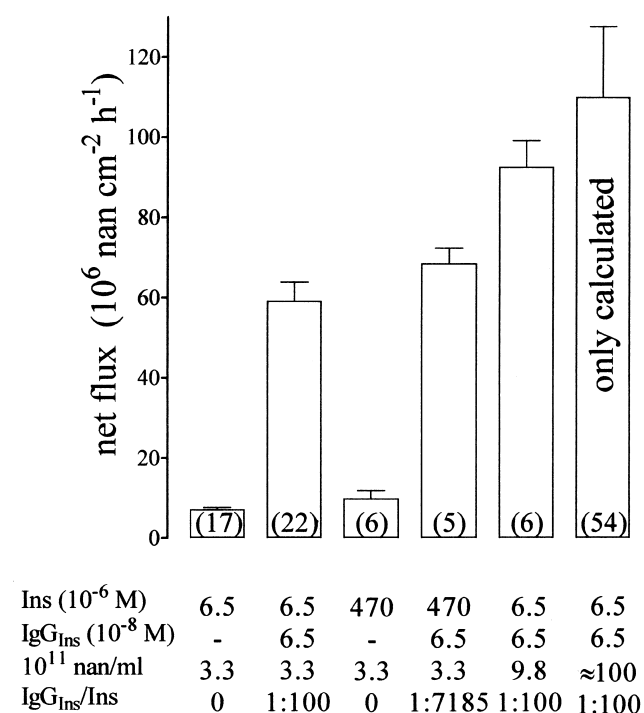


Fig. 4. Maximal transport capacity of the endocytotic process reached by stimulating the transport of insulin-coated nanospheres with anti-insulin IgG: net flux stimulation obtained under different conditions. The results are presented as mean \pm S.E.M. (number of experiment in brackets).

here used, namely 27°C). The Van 't Hoff coefficient (Q_{10}), measured between 27 and 37°C, is 2.2 [6] so that per se the transport at 34°C would increase to about $156 \cdot 10^6$ nan $\text{cm}^{-2} \text{h}^{-1}$. However, the observed crowding and aggregation of nanospheres, suggesting saturation of the exits from the epithelium, makes this increase unlikely, at least to this extent.

Finally, it is to emphasize that this maximal transport is a mean transfer per hour based on the overall transport measured over 2 h. We have previously shown that a transport peak occurs during the first 30 min, followed by a slow decrease during the subsequent 90 min [1].

4.3. Percentage of polypeptide-transporting cells in the upper concha epithelium

On this basis it is possible to calculate the percentage of polypeptide-transporting cells in the upper concha epithelium.

It can reasonably be assumed that: (i) transcytotic cycle length, included the time of release into the

submucosal medium, is about 1.5 min, (ii) one transporting cell concomitantly handles about 10 beads per cycle, as a mean for the cycles occurring in an hour under maximal transport conditions.

As for statement (i), in a previous paper [1] we showed that in nasal mucosa, if active polypeptide transport is measured every 15 min, the maximal transport is already achieved during the first 15 min period. In intestinal Peyer's patches, where transport was measured every 5 min, the maximal transport was already present during the first 5 min period [11]. Thus the transcytotic cycle in all these epithelial cells should last much less than 5 min, say 1–2 min. Consistently with this estimate, the matter entering the cell by endocytosis is known generally to be internalized and found in early endosomes in 20 s; the subsequent part of the process lasts for different periods, depending on the cells and the different steps required by the function performed by endocytosis [13]. In a transcytosis, after the formation of the endocytic carrier vesicles (ECV) from early endosomes, a rapid movement of ECV along the microtubules is the only step required before basolateral exocytosis; the ECV movement rate can be $5 \mu\text{m s}^{-1}$. Therefore, even if the length of the cytoplasm to be crossed corresponds to the entire transporting epithelium length ($45 \mu\text{m}$: [7]), the time required would be 9 s. Taking into account the time for the exocytotic process and diffusion out of the cell along unstirred layers, 1.5 min is a sufficiently reliable value.

As for statement (ii), in nasal mucosa approx. 20 nanospheres were bound on the apical membrane of M-cells [7]. Since the uptake/binding ratio is about 0.5 in intestinal M-cells [10], about 10 beads are likely to be transported per nasal M-cell.

If so, each transporting cell can perform about 40 cycles and handle 400 nanoparticles per hour. Hence, considering $90 \cdot 10^6$ nan $\text{cm}^{-2} \text{h}^{-1}$ as the actual maximal transport capacity, the number of transporting cells should be $225 \cdot 10^3 \text{ cm}^{-2}$. On the basis of unpublished data accumulated during the preparation of previous histo-physiological papers [5,7], we can state that: (i) the mean cell diameter in the upper concha epithelium is $5 \mu\text{m}$, so that the surface area per cell is approx. $20 \mu\text{m}^2$, (ii) owing to small plications the actual epithelial area is $1.3 \times$ the apparent area. Thus $6.5 \cdot 10^6$ cells are present per cm^2 of apparent area, and the transporting cells under maximal trans-

port conditions correspond to about 3.5%. Apparently this value is in agreement with the lowest values reported for the follicle-associated epithelium (FAE) of mouse Peyer's patches, where M-cells represent 1.6–10.9% of cells (depending on FAE region) in germ-free animals, and increase to 5.4–21.0% in antigen-stimulated animals [14]. However, the calculated value of 3.5% transporting cells in nasal mucosa refers to the overall epithelium as opposed to areas specializing in this transport only; thus it may even seem rather high. Nevertheless, it must be emphasized that: (i) in rabbit FAE, M-cells reach much higher percentages than in mouse FAE (M.W. Smith, personal communication), (ii) the animals examined for this paper were not germ- or pathogen-free animals, but exposed to the mean antigen charge of a normal animal house.

The calculated value of transporting cells cannot be affected by the *in vivo* higher temperature of the epithelium, as the increase in maximal transport across the tissue (which however is unlikely, for the reasons reported above) is due to an increase in transport per cell.

Finally, it is to emphasize that all the calculations reported above are on mean values of transport per cell, independently of possible differences in efficiency of the transporting cells.

4.4. Kinetics of active and passive fluxes

The net (active) transport as a function of bead concentration (with constant coating) follows sigmoidal kinetics, with a low Hill number (1.5). Sigmoidal kinetics with a high Hill number (3.3) has previously been found for transport of carbocalcitonin-coated beads as a function of carbocalcitonin coating [6]; in this case the easy interpretation was that the formation of binding between nanoparticle and receptor facilitates two more bindings of the same nanoparticle with other two receptors of the same coated pit, thus strengthening the probability of transport; of course, the probability of involvement of many bindings increases with the extent of coating per nanosphere [6]. Conversely, in the experiments reported here increasing bead concentration creates competition, not cooperation for the pit. Then, the sigmoidal kinetics here shown can be related either to the presence and recruitment of many different receptors

with different affinities for IgG (and different cross-affinities for other polypeptides) or to different affinities (frequent with a random distribution) between IgG and the same type of receptor; the different affinities may be related to the possible slightly different orientations of the IgG molecules bound to the adsorbed insulin molecules.

The passive flux J_{sm} already displays saturation with a $2 \cdot 10^9$ nan/ml concentration. Thus it is not only independent of bead coating and so crosses the epithelium through non-specific pathways, but also moves by restricted, probably single-file diffusion. Hence the nanolesions involved have probable diameters of about 500 nm; in any event there must be very few of them to permit the low J_{sm} observed and the maintenance of a substantial transepithelial potential difference.

4.5. Final comments

On the background that nasal application of polypeptide hormones and related active principles is a therapeutic strategy one might speculate that conjugation of these polypeptides to antibodies might increase the absorption and thus bioavailability of these substances.

Acknowledgements

This research received financial support from ACRAF Angelini Ricerche, S. Palomba Pomezia, Roma.

References

- [1] D. Cremaschi, C. Rossetti, M.T. Draghetti, C. Manzoni, V. Aliverti, Active transport of polypeptides in the rabbit nasal mucosa: possible role in the sampling of potential antigens, *Eur. J. Physiol. (Pflügers Arch.)* 419 (1991) 425–432.
- [2] D. Cremaschi, C. Porta, R. Ghirardelli, C. Manzoni, I. Caremi, Endocytosis inhibitors abolish the active transport of polypeptides in the mucosa of the nasal upper concha of the rabbit, *Biochim. Biophys. Acta* 1280 (1996) 27–33.
- [3] D. Cremaschi, C. Porta, R. Ghirardelli, The active transport of polypeptides in the rabbit nasal mucosa is supported by a specific vesicular transport inhibited by cytochalasin D, *Biochim. Biophys. Acta* 1283 (1996) 101–105.
- [4] D. Cremaschi, C. Porta, R. Ghirardelli, Endocytosis of poly-

- peptides in the nasal respiratory mucosa of the rabbit, *News Physiol. Sci.* 12 (1997) 219–225.
- [5] D. Cremaschi, R. Ghirardelli, C. Porta, Relationship between polypeptide transcytosis and lymphoid tissue in the rabbit nasal mucosa, *Biochim. Biophys. Acta* 1369 (1998) 287–294.
- [6] D. Cremaschi, C. Porta, R. Ghirardelli, Different kinds of polypeptides and polypeptide-coated nanoparticles are accepted by the selective transcytosis shown in the rabbit nasal mucosa, *Biochim. Biophys. Acta* 1416 (1999) 31–38.
- [7] R. Ghirardelli, F. Bonasoro, C. Porta, D. Cremaschi, Identification of particular epithelial areas and cells that transport polypeptide-coated nanoparticles in the nasal respiratory mucosa of the rabbit, *Biochim. Biophys. Acta* 1416 (1999) 39–47.
- [8] R. Weltzin, P. Lucia-Jandris, P. Michetti, B.N. Fields, J.P. Kraehenbuhl, M.R. Neutra, Binding and transepithelial transport of immunoglobulins by intestinal M cells: demonstration using monoclonal IgA antibodies against viral proteins, *J. Cell Biol.* 108 (1989) 1673–1685.
- [9] J. Pappo, T.H. Ermak, H.J. Steger, Monoclonal antibody-directed targeting of fluorescent polystyrene microspheres to Peyer's patch M cells, *Immunology* 73 (1991) 277–280.
- [10] C. Porta, P.S. James, A.D. Phillips, T.C. Savidge, M.W. Smith, D. Cremaschi, Confocal analysis of fluorescent bead uptake by mouse Peyer's patch follicle-associated cells, *Exp. Physiol.* 77 (1992) 929–932.
- [11] M.W. Smith, N.W. Thomas, P.G. Jenkins, N.G.A. Miller, D. Cremaschi, C. Porta, Selective transport of microparticles across Peyer's patch follicle-associated M cells from mice and rats, *Exp. Physiol.* 80 (1995) 735–743.
- [12] D. Cremaschi, C. Rossetti, M.T. Draghetti, C. Manzoni, C. Porta, V. Aliverti, Transepithelial electrophysiological parameters in rabbit respiratory nasal mucosa isolated 'in vitro', *Comp. Biochem. Physiol.* 99A (1991) 361–364.
- [13] I. Pastan, M.C. Willingham, The pathway of endocytosis, in: I. Pastan, M.C. Willingham (Eds.), *Endocytosis*, Plenum Press, New York, 1985, pp. 1–40.
- [14] T.C. Savidge, M.W. Smith, P.S. James, P. Aldred, Salmonella-induced M-cells formation in germ-free mouse Peyer's patch tissue, *Am. J. Pathol.* 139 (1991) 177–184.